How bad is the rain? Applying the extreme rain multiplier globally and for climate monitoring activities

Received: 16 September 2024 | Revised: 10 January 2025 | Accepted: 1 February 2025

DOI: 10.1002/met.70031

RESEARCH ARTICLE

Meteorological Applications
Science and Technology for Weather and Climate
Open Access
RMetS

How bad is the rain? Applying the extreme rain multiplier globally and for climate monitoring activities

David A. Lavers[1,2] | **Gabriele Villarini**[3,4] | **Hannah L. Cloke**[5,6] | **Adrian Simmons**[1] | **Nigel Roberts**[1] | **Anna Lombardi**[1] | **Samantha N. Burgess**[1] | **Florian Pappenberger**[1]

[1]European Centre for Medium-Range Weather Forecasts (ECMWF), Reading, UK

[2]School of Geography, Earth and Environmental Sciences, University of Birmingham, Birmingham, UK

[3]Department of Civil and Environmental Engineering, Princeton University, Princeton, New Jersey, USA

[4]High Meadows Environmental Institute, Princeton University, Princeton, New Jersey, USA

[5]Department of Geography and Environmental Science, University of Reading, Reading, UK

[6]Department of Meteorology, University of Reading, Reading, UK

Correspondence
David A. Lavers, European Centre for Medium-Range Weather Forecasts (ECMWF), Shinfield Park, Reading, RG2 9AX, UK.
Email: david.lavers@ecmwf.int

Funding information
Natural Environment Research Council, Grant/Award Number: NE/S015590/1; Copernicus Climate Change Service

Abstract

A typical question posed following an extreme precipitation event is: How does this compare to past events? This question is being asked more frequently and is of importance to climate monitoring services, such as the Copernicus Climate Change Service (C3S). Currently, the statistics extensively used for this purpose are not generally understandable to the wider public, or they are not tailored towards presenting extremes. To mitigate this situation, this article uses a modified version of the Extreme Rain Multiplier (ERM), which was developed for tropical cyclones, and applies it to precipitation events globally. For daily precipitation considered herein, the ERM is calculated by dividing the daily precipitation accumulation during an event by the mean historical annual maxima of daily precipitation (RX1day), which is computed over 1991–2020. Using the European Centre for Medium-Range Weather Forecasts ERA5 reanalysis, the calculation of the ERM is illustrated for six extreme events around the world; these included convective systems, atmospheric rivers and tropical cyclones. A maximum ERM of 4 was found during Storm Daniel, in Greece, and in Tropical Cyclone Jasper in Australia, implying that four times the mean RX1day precipitation occurred. The ERM will be useful in C3S reporting activities because it can objectively identify extreme precipitation events. Furthermore, after extracting the number of precipitation events per year at each grid point that had an ERM exceeding 1, a trend analysis was undertaken to ascertain if the frequency of extreme events had changed with time. Results showed that the most widespread increasing trends in the ERM

were in the tropics, but these trends are thought to be questionable in ERA5. There were few clear trends in other regions. In conclusion, the ERM can communicate the level of extreme precipitation in a clear manner and can be used in climate monitoring activities.

KEYWORDS

communication, ERA5 precipitation, extreme events, extreme rain multiplier

1 | INTRODUCTION

After an extreme precipitation event, a common question arises: How does this compare to past events? Journalists, decision-makers, policymakers and responders are asking this question with increasing frequency. This trend is driven not only by a recent surge in severe weather events but also by a growing recognition of the impact of climate change on weather patterns. The topic is also of major importance to climate monitoring services, such as the Copernicus Climate Change Service (C3S; Buontempo et al., 2022), due to the need for clear communication of the Earth's changing climate to the media, decision-makers and the public, and because of the large socio-economic impacts of these events. In the climate monitoring activities of C3S, in particular the monthly bulletins (https://climate.copernicus.eu/climate-bulletins) and annual European State of the Climate (ESOTC) report (https://climate.copernicus.eu/ESOTC), it is usual for mean anomalies of precipitation with respect to a historical reference period to be presented, which can be used to identify extreme events when they heavily influence the mean. However, these products are not tailored towards presenting information about extremes.

There are a few techniques currently used to communicate the climatological context of extremes, as outlined below.

First, the return period—a statistic widely used in engineering, including in dam construction—is employed. It describes a certain event as having a probability of occurring or being exceeded in each year. For example, a precipitation event with an annual exceedance probability of 0.01, or a 1% chance of occurring in any given year, is referred to as having a 1-in-100-year return period. However, using the return period terminology can be problematic for the communication of extremes because it is often misinterpreted as an event that happens exactly once every 100 years, which leads to a false sense of security if an event happened a short time ago, because it is anticipated to be a long time until the next one. In turn, there is ineffective communication about the nature and magnitude of the risks and potentially inadequate preparation is made for such events (Lave & Lave, 1991). Further issues with return periods include their limited transferability to other nearby locations, uncertainties associated with their estimation, and the assumption of stationarity which is no longer valid due to changes in climate (e.g., Kim & Villarini, 2024; Salas & Obeysekera, 2014) and the built environment.

The second technique used to describe extreme events is the number of standard deviations from the mean (Thompson et al., 2022; You et al., 2024). While this classification may be appropriate to a scientific audience, the use of standard deviations is not readily understandable to the wider public.

The third approach is to characterize an extreme precipitation event as the percentage of the expected annual, seasonal or monthly total precipitation. This method of using percentages can be seen occasionally in the broadcast media, in output from national meteorological services (e.g., the UK Met Office; https://blog.metoffice.gov.uk/2024/05/01/a-wet-and-dull-april/), and in the monthly hydrological summaries of the UK National Hydrological Monitoring Programme (NHMP; https://nrfa.ceh.ac.uk/monthly-hydrological-summary-uk). A limitation of using a percentage approach, however, is that it does not present an event in the context of past extreme events.

A further metric specifically developed for characterizing tropical cyclone rainfall is the Extreme Rain Multiplier (ERM; Bosma et al., 2020), which presents a rainfall event as the ratio of the local climatological 2-year rainfall value. The ERM was shown by Bosma et al. (2020) to produce values corresponding to observed tropical cyclone impacts, thus identifying hazardous events, and to afford the opportunity for people to relate the magnitude of precipitation events to those typically experienced in a region. These properties mean that the ERM could have strong potential for communicating extreme precipitation events. The aim of this article is to investigate further the ERM for communicating extreme precipitation by extending the reach of the earlier findings of Bosma et al. (2020) by (1) applying a modified version of the ERM to events around the globe and not just to tropical cyclones in the United States, (2) discussing possible applications for climate monitoring activities, and (3) investigating trends in the ERM metric over time around the world.

2 | DATA AND METHODS

2.1 | The ERA5 reanalysis

The ERA5 reanalysis (Hersbach et al., 2020) from the European Centre for Medium-Range Weather Forecasts (ECMWF) was used for this study because it is widely employed in C3S climate monitoring activities. ERA5 provides a comprehensive record of the global atmosphere, land surface and ocean waves on a 31-km (TL639) horizontal grid; and the system is based on the ECMWF Integrated Forecasting System (IFS) Cy41r2. Four daily ERA5 precipitation accumulations (0000 UTC to 0000 UTC; 0600 UTC to 0600 UTC; 1200 UTC to 1200 UTC; and 1800 UTC to 1800 UTC) were extracted from the ECMWF archive—and interpolated on to a regular 0.25° × 0.25° grid—from 1 January 1979 to 31 December 2023. These four overlapping daily, or 24-h, accumulations were used to capture more of the entirety of daily extreme precipitation events because using one non-overlapping period, such as 0000 UTC to 0000 UTC, would not capture all of the precipitation in an event that straddled 0000 UTC. The 1979–2023 period was chosen as there is more confidence in ERA5 precipitation during the satellite era since 1979. The precipitation fields are also available in the C3S Climate Data Store (https://cds.climate.copernicus.eu). ERA5 precipitation is generally more skillful in the Extratropics compared with the Tropics, which is partly due to the difficulty ERA5 has in resolving convective processes in the Tropics on its relatively coarse model grid. In terms of extremes, the precipitation patterns from ERA5 and the observations broadly agree, but ERA5 has issues capturing the highest observed precipitation totals (e.g., Lavers et al., 2022).

2.2 | The extreme rain multiplier

To determine how extreme an event is we need to calculate how different it is compared with climatological conditions. The standard practice used to place current climate conditions in their climatological context is to apply a 30-year climate average or reference period; currently, 1991–2020 is recommended by the World Meteorological Organization. C3S uses the 1991–2020 reference period in its regular monitoring products, and the ERM approach of Bosma et al. (2020) is also built using a reference period; in their case, it was 1981–2010. We now define the ERM for daily precipitation.

The ERM metric is calculated by dividing the 24-h precipitation accumulation P during an event by the mean historical annual maxima of 24-h precipitation (RX1day) (Zhang et al., 2011) at a given location:

$$\mathrm{ERM} = \frac{P_t}{\boldsymbol{RXtday}} \tag{1}$$

where t is the accumulation period (i.e., 24 h herein). To calculate the mean RX1day, for each of the 30 years in the 1991–2020 reference period, we extracted the maximum 24-h precipitation out of the four 24-h accumulation periods (0000 UTC to 0000 UTC; 0600 UTC to 0600 UTC; 1200 UTC to 1200 UTC; and 1800 UTC to 1800 UTC), and then the mean of the 30 values was computed at each grid point. This version of the ERM is modified from Bosma et al. (2020) in two key ways. First, the RX1day statistics are built using four overlapping daily periods, rather than solely the 1200 UTC to 1200 UTC as in Bosma et al. (2020), providing a more accurate and hence robust estimate of the historical annual maxima. Figure 1 illustrates this point by showing the mean RX1day values gradually increasing with the inclusion of additional daily periods, and this is noticeable, for example, over Europe and the southern United States (cf. Figure 1a,d). Second, the mean RX1day is used as opposed to the median RX1day because the mean is considered more widely understood for communication purposes. In Figure 2, the median historical annual maxima (Figure 2a), the mean historical annual maxima (Figure 2b) and the mean minus median values (Figure 2c) are plotted. This shows that the largest differences between the two estimates are mostly confined to tropical regions and especially ocean areas where tropical cyclones occur (e.g., to the southeast of Florida), while differences in the mid-latitudes are generally small. Note that higher uncertainty exists in the estimate of the mean in tropical regions, in part due to issues with ERA5 precipitation there, which is in line with the results of Lavers et al. (2022) and Kumar et al. (2024). Arid regions, such as areas in northern Africa, also have higher uncertainty due to the few extreme events that occur.

The ERM is closely related to a technique employed in the 2022 State of the Climate Report of the Bulletin of the American Meteorological Society (Blunden et al., 2023), but in that report, P was the RX1day precipitation for 2022 as opposed to a particular event accumulation and the resulting ratio was presented as a percentage. Mazzoglio et al. (2020) proposed a similar index, the Normalized Maximum Value, which compared the maximum precipitation value at a station with the mean annual precipitation (or local climatology). A similar method has also been used to normalize flood peaks across river basins of varied sizes (Smith et al., 2018;

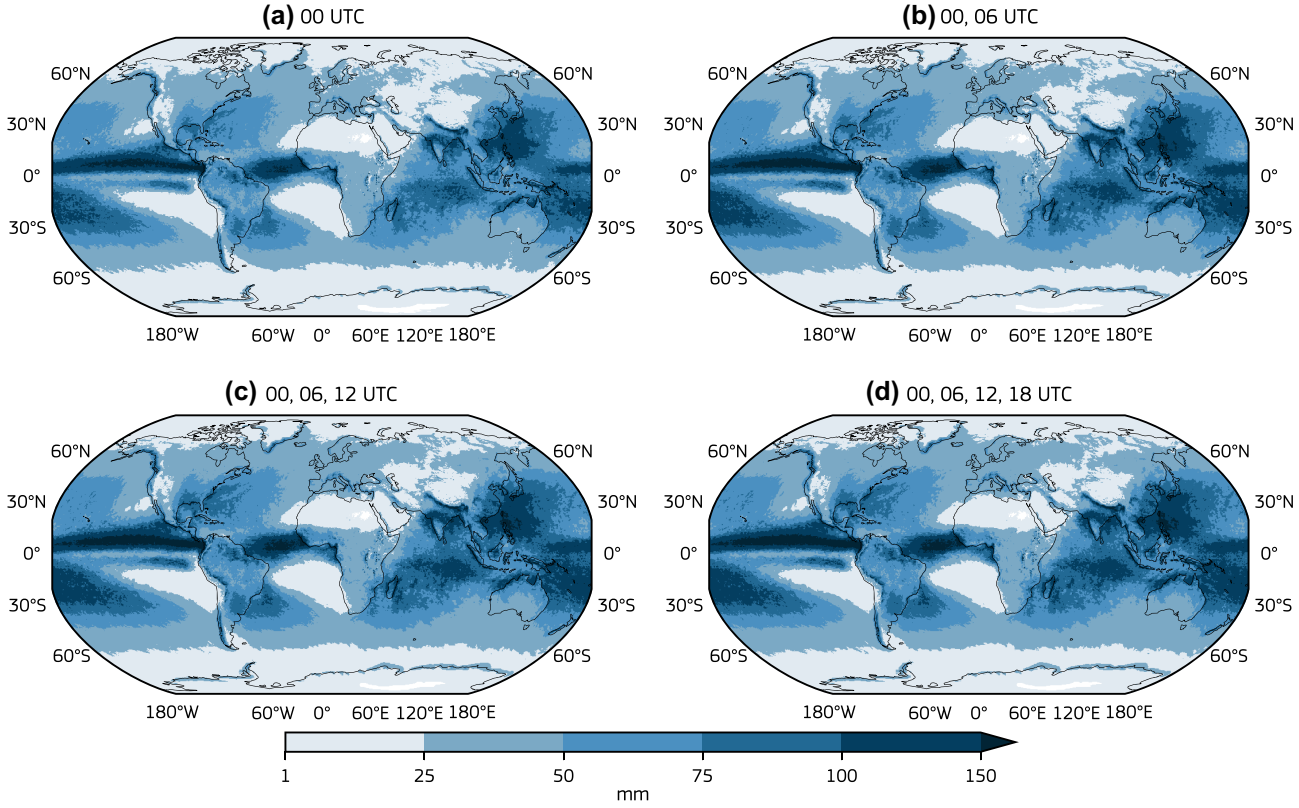

FIGURE 1 The mean RX1day in ERA5 across 1991–2020 built using (a) the 0000 UTC to 0000 UTC 24-hour precipitation accumulation period, (b) the 0000 UTC to 0000 UTC and 0600 UTC to 0600 UTC 24-hour precipitation accumulation periods, (c) the 0000 UTC to 0000 UTC, 0600 UTC to 0600 UTC, and the 1200 UTC to 1200 UTC 24-hour precipitation accumulation periods, and (d) 0000 UTC to 0000 UTC, 0600 UTC to 0600 UTC, 1200 UTC to 1200 UTC, and 1800 UTC to 1800 UTC 24-hour precipitation accumulation periods. White areas over northeast Africa and Antarctica indicate areas with values below 1 mm.

Villarini et al., 2014), but in those studies, the 10-year flood was used as a benchmark and not the mean.

2.3 | Trend analysis with Poisson regression

The identification of extreme precipitation events with the ERM affords an opportunity to evaluate if their frequency has changed across 1979–2023, or the satellite era, a period when there is more confidence in ERA5 precipitation. To undertake this trend assessment, Poisson regression is employed, which is a form of regression in which the response variable is in the form of count data and follows a Poisson distribution. Herein, the count data are the number of precipitation events per year at each grid point with an ERM >1 (i.e., values greater than the mean RX1day), and these are modelled as a function of time, or year, to determine whether there is a trend. If N_i is the number of events in each year i for a particular accumulation period (e.g., 0000 UTC to 0000 UTC), then N_i is described by a conditional Poisson distribution with parameter λ_i. The relationship between the parameter λ_i and the covariate is assumed to be linear (via a log-link function):

$$\lambda_i = exp[\beta_0 + \beta_1 z_{1i}] \quad (2)$$

where z_{1i} is the ith year in a vector of years 1979–2023. Increasing or decreasing trends in the number of extreme events are identified at grid points where the p-value of the β_1 coefficient is <0.05.

3 | RESULTS

3.1 | ERM examples around the globe

Six extreme precipitation events are used to illustrate the ERM. First, for three extreme events in Europe, Figure 3 shows the mean RX1day in the region affected in the left column (Figure 3a,d,g), the daily ERA5 precipitation accumulations in the middle column (Figure 3b,e,h), and the ERM in the right column (Figure 3c,f,i), which is

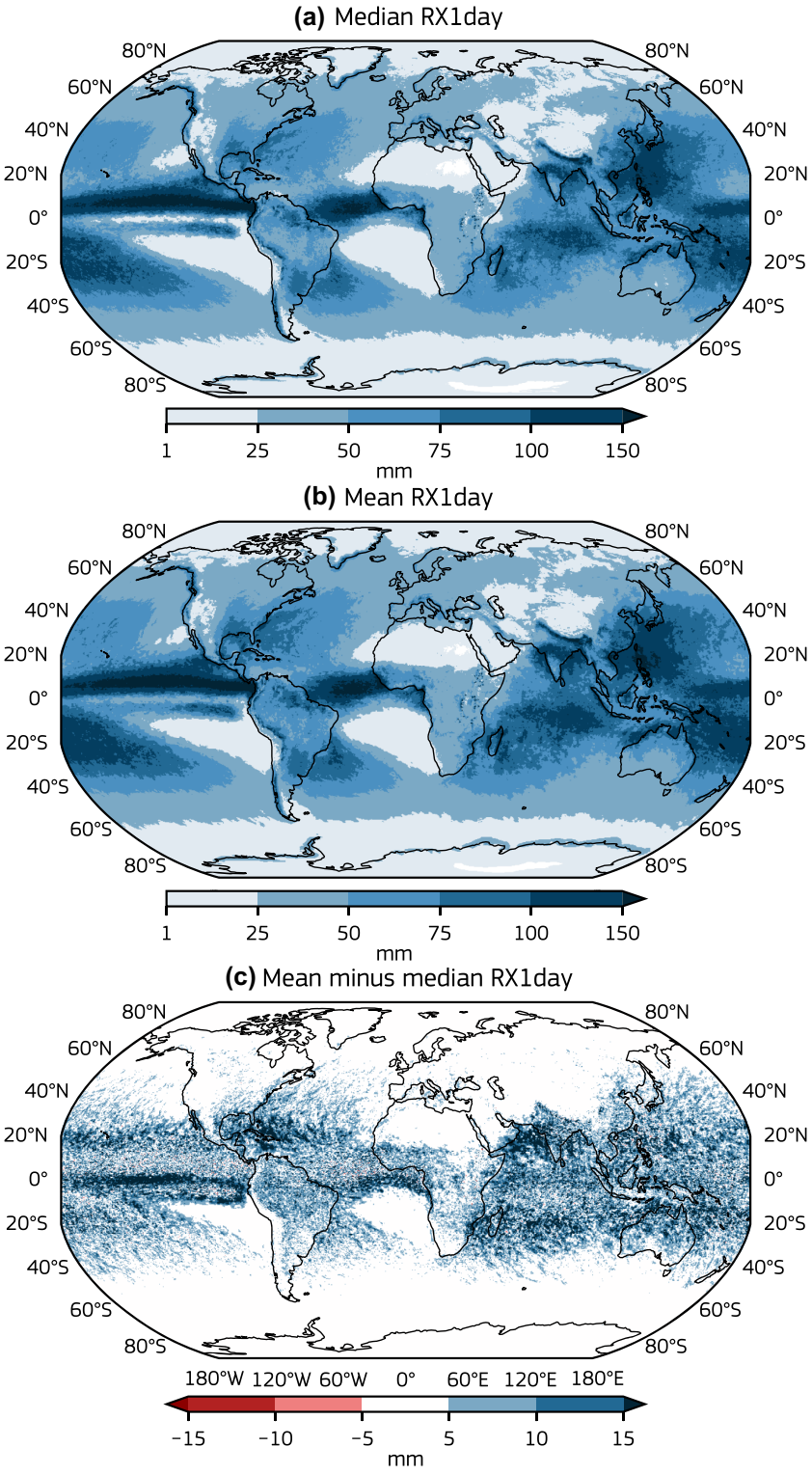

FIGURE 2 The (a) median and (b) mean RX1day in ERA5 across 1991–2020 built using the 0000 UTC to 0000 UTC, 0600 UTC to 0600 UTC, 1200 UTC to 1200 UTC, and 1800 UTC to 1800 UTC 24-hour precipitation accumulation periods. White areas over northeast Africa and Antarctica indicate areas with values below 1 mm. (c) The difference between the mean and median RX1day.

computed by dividing the fields in the middle column by those in the left column. For 14 July 2021—an event that led to devasting flooding and more than 200 fatalities in parts of Belgium, Germany, and surrounding countries—it is shown that an ERM of 3 occurred over northwest Germany (Figure 3c), which implies that the daily precipitation accumulation of around 100 mm was at least three times the mean RX1day. In Scandinavia on 13 January 2022, an atmospheric river (Ralph et al., 2018) led to widespread precipitation values of between 50 and 75 mm and resulted in an ERM of around 1.5 in parts of Norway and Sweden (Figure 3f); this indicates that values above the mean RX1day occurred. Lastly, from 5 to 6 September 2023, Storm Daniel caused precipitation

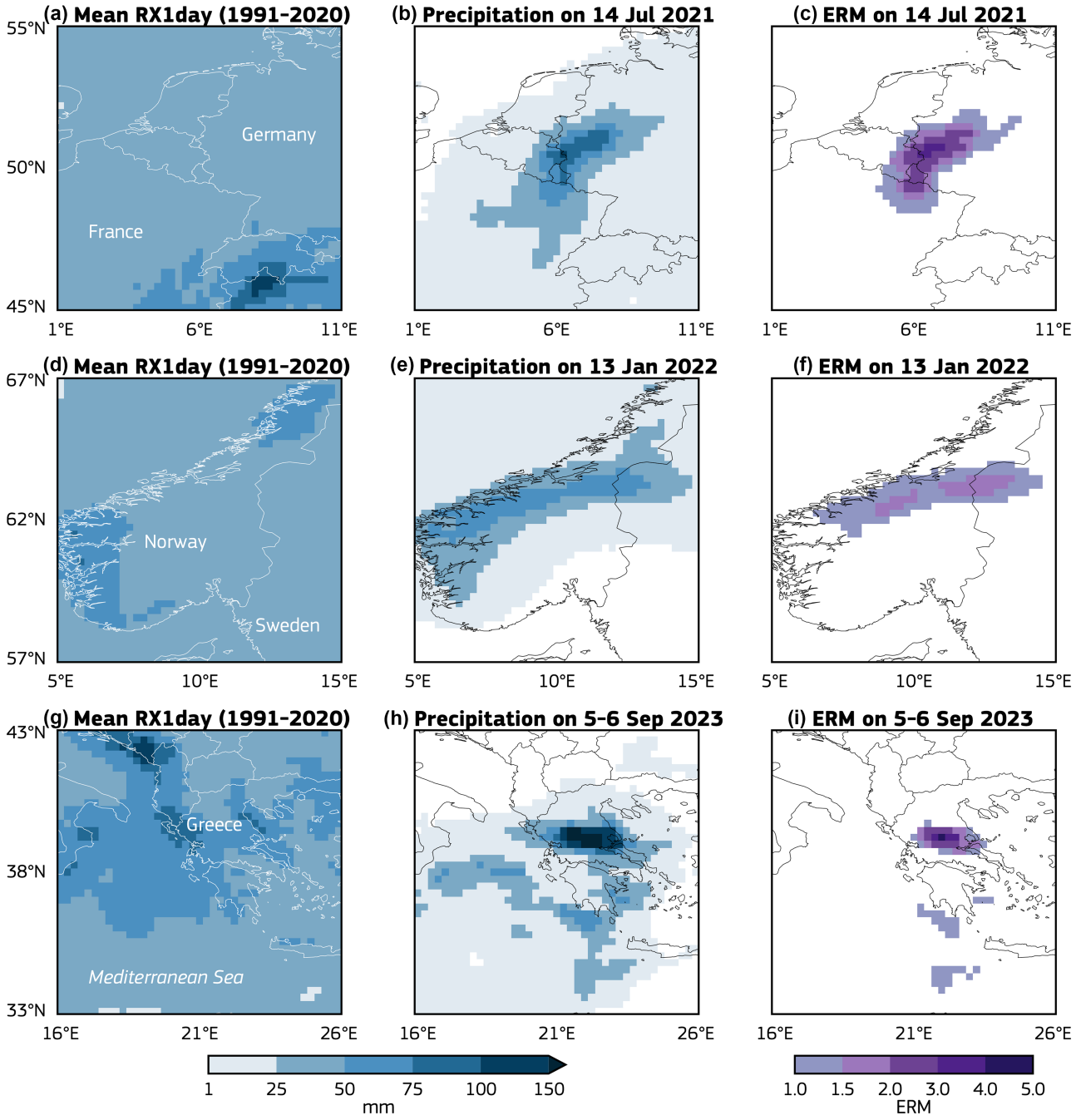

FIGURE 3 Examples of the Extreme Rain Multiplier (ERM) across Europe. (a, d, g) The mean RX1day in ERA5 across 1991–2020. (b, e, h) Daily precipitation accumulations in ERA5 from 0000 UTC 14 July 2021 to 0000 UTC 15 July 2021, from 0000 UTC 13 January 2022 to 0000 UTC 14 January 2022, and from 1800 UTC 5 September 2023 to 1800 UTC 6 September 2023. (c, f, i) The ERM for presenting the historical context of the extreme precipitation in the three events. Note that white colours in the middle column (b, e, h) indicate areas with precipitation below 1 mm.

values between 100 and 200 mm across the Thessalian Plain in Greece, which translated into an ERM of 4 at one grid point, or at least four times the mean RX1day over a part of Greece (Figure 3i).

Second, three global events are presented in terms of the ERM in Figure 4: (1) Hurricane Ian over Florida on 28 September 2022 (Figure 4a–c), which was located in the same domain as assessed by Bosma et al. (2020); (2) Tropical Cyclone Jasper over Australia from 16 to 17 December 2023 (Figure 4d–f); and (3) an atmospheric river across California on 5 February 2024 (Figure 4g–i). For Hurricane Ian and Tropical Cyclone Jasper, precipitation accumulations of over 150 mm were estimated, which corresponded to ERMs of 3 and 4 at a few grid

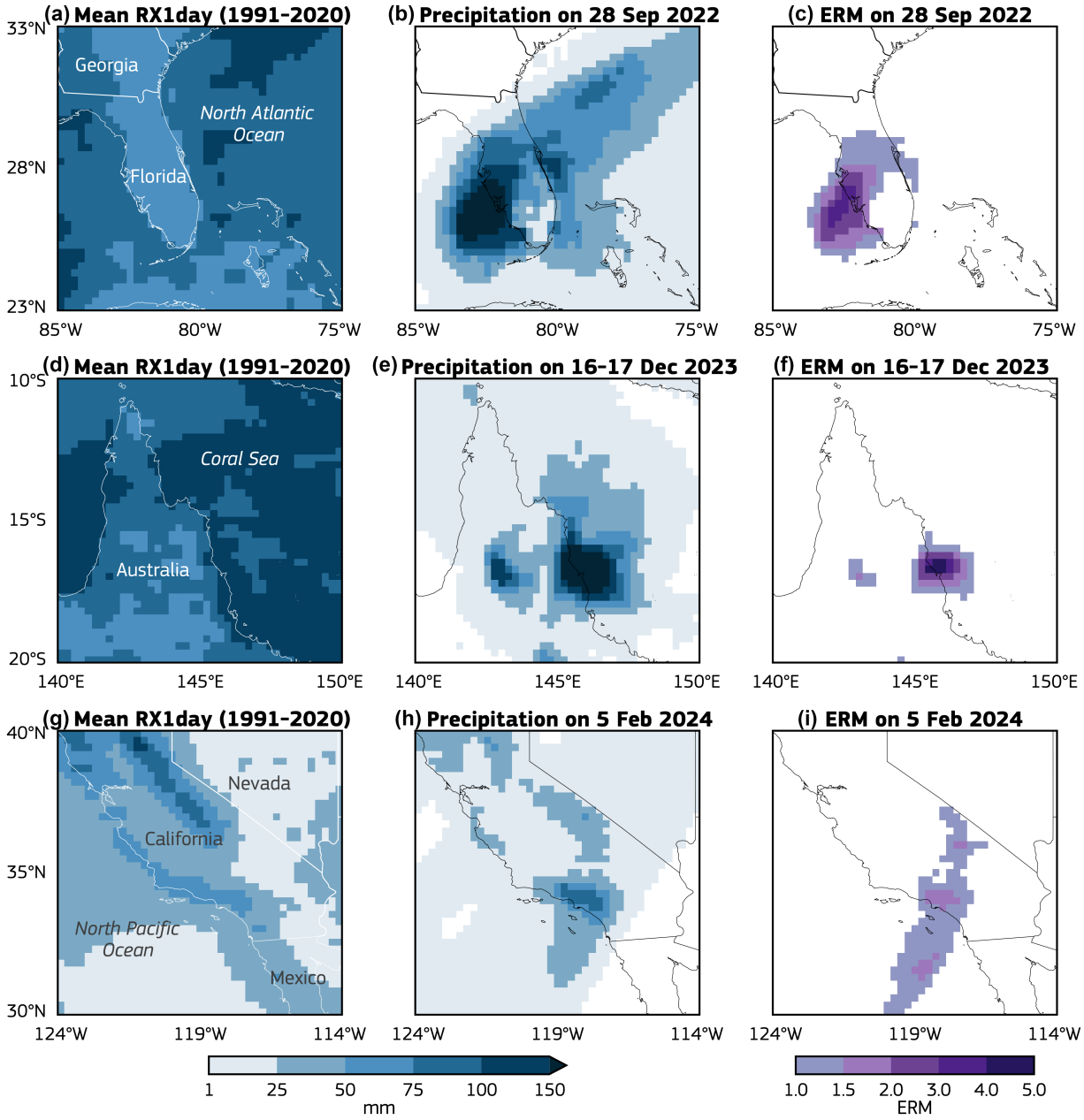

FIGURE 4 Examples of the Extreme Rain Multiplier (ERM) across the globe. (a, d, g) The mean RX1day in ERA5 across 1991–2020. (b, e, h) Daily precipitation accumulations in ERA5 from 0000 UTC 28 September 2022 to 0000 UTC 29 September 2022, from 1800UTC 16 December 2023 to 1800UTC 17 December 2023, and from 0000 UTC 5 February 2024 to 0000 UTC 6 February 2024. (c, f, i) The ERM for presenting the historical context of the extreme precipitation in the three events. Note that white colours in the middle column (b, e, h) indicate areas with precipitation below 1 mm.

points or three and four times the mean RX1day precipitation, respectively. The final event that chiefly affected the Transverse Ranges in California was between 75 and 100 mm, with many grid points having an ERM greater than 1, or values exceeding the mean RX1day precipitation.

A comparison is now made between the revised ERM in Figures 3 and 4 and the original Bosma et al. (2020) method. Building the RX1day statistics with only the 1200 UTC to 1200 UTC 24-h accumulation period and computing the median RX1day, rather than the mean RX1day, Figures S1 and S2 present the six extreme precipitation events with the Bosma et al. (2020) approach. Two notable differences can be seen. Larger climatological RX1day precipitation values are found, which arise in part from the use of four overlapping periods (cf. Figure 3a,d,g with Figure S1a,d,g; Figure 4a,d,g with Figure S2a,d,g). This suggests that the historical annual maxima are better sampled with the revised ERM applied herein. The use of the mean also leads, in most places, to larger values because precipitation tends to have a skewed distribution. Moreover, this comparison indicates

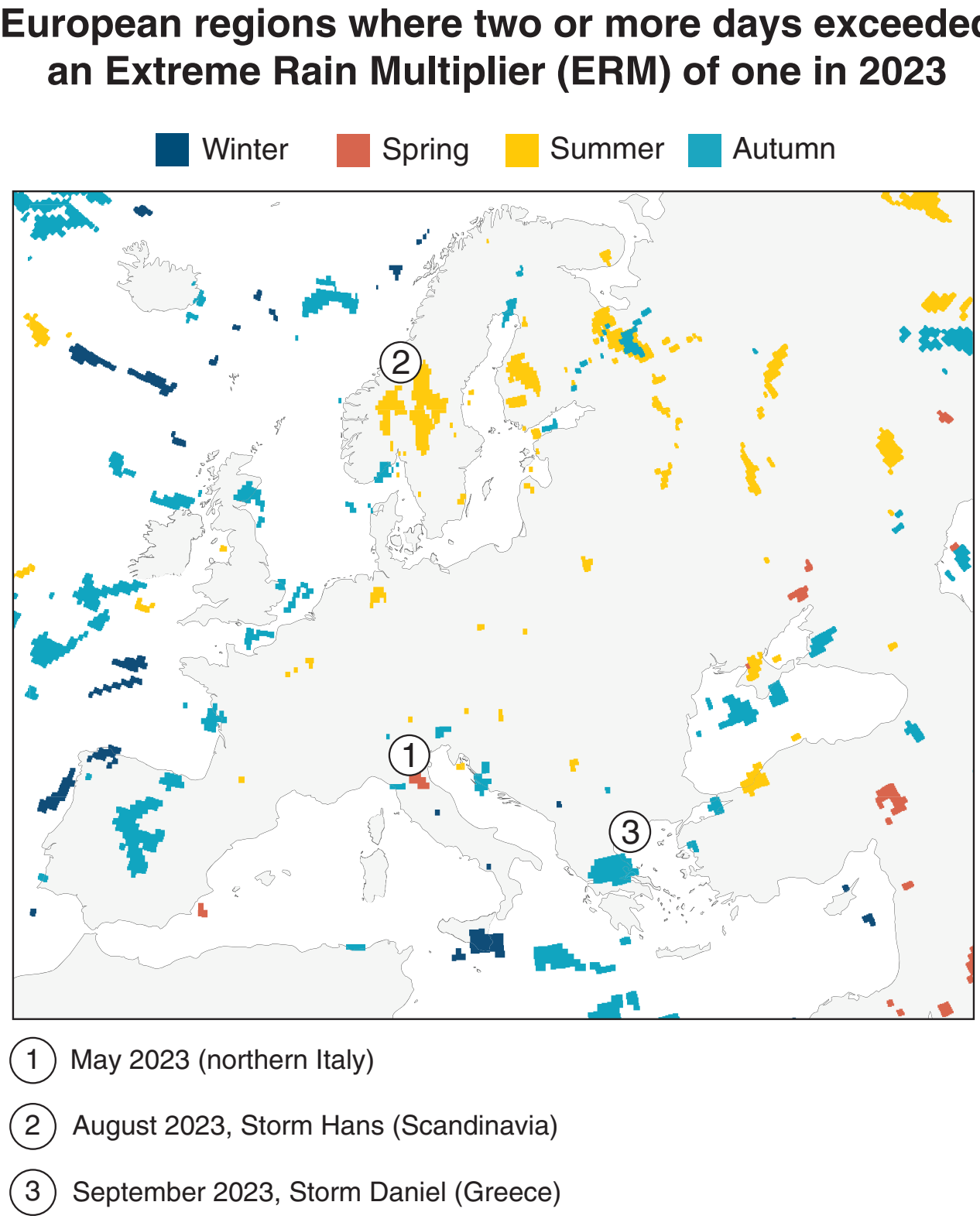

FIGURE 5 European regions where two or more days (using the 0000 UTC to 0000 UTC accumulation period) exceeded an Extreme Rain Multiplier (ERM) of one in winter (December, January and February), spring (March, April and May), summer (June, July and August), and autumn (September, October and November) 2023. Winter relates to December 2022–February 2023. Three extreme precipitation (and flooding) events are highlighted.

that the revised ERM is more able to isolate the actual areas affected by extreme precipitation, and this is seen by the smaller ERM areas identified in the examples presented (cf. Figure 3c,f,i with Figure S1c,f,i; Figure 4c,f,i with Figure S2c,f,i).

The ERM maps in Figures 3 and 4 highlight the location and signify the extreme nature of the precipitation events which may help to communicate more clearly the level of extreme precipitation to the media and the public. One aspect to note with the ERA5 precipitation herein is that the precipitation values are likely to be less than those observed, in part owing to the coarse IFS model grid used in ERA5. A preliminary investigation, however, using RX1day precipitation from a previous study (Lavers et al., 2022) suggests that the general low bias of ERA5 extreme precipitation is removed when viewed as the ERM.

3.2 | Application of the ERM for climate monitoring activities

As well as conveying the extreme nature of events, the ERM could also have further uses in climate monitoring activities, such as in the annual C3S ESOTC report. For example, by counting and then visualizing the number of precipitation events exceeding a certain ERM threshold, it is possible to identify extreme events objectively, rather than subjectively based on, for instance, media reports. This would then allow for further investigation of events of particular interest. Figure 5 illustrates how these data could be visualized by showing regions where two or more (not necessarily consecutive) days in each season in 2023 exceeded an ERM of one. This graphic clearly identifies areas affected by extreme precipitation, and three known events are highlighted: (1) a wet period in Italy during the first half of May 2023; (2) Storm Hans in Scandinavia in August 2023; and (3) Storm Daniel in Greece in September 2023 (see also Figure 3g–i). These events were discussed in the 2023 ESOTC report (https://climate.copernicus.eu/esotc/2023). It is also possible that such a graphic as shown in Figure 5 could be used to determine, at least qualitatively, if extreme events were more numerous and/or widespread than in previous years, as discussed quantitatively in the next section.

3.3 | Trend analysis with Poisson regression

The identification of extreme events with the ERM presents an opportunity to evaluate if the frequency of

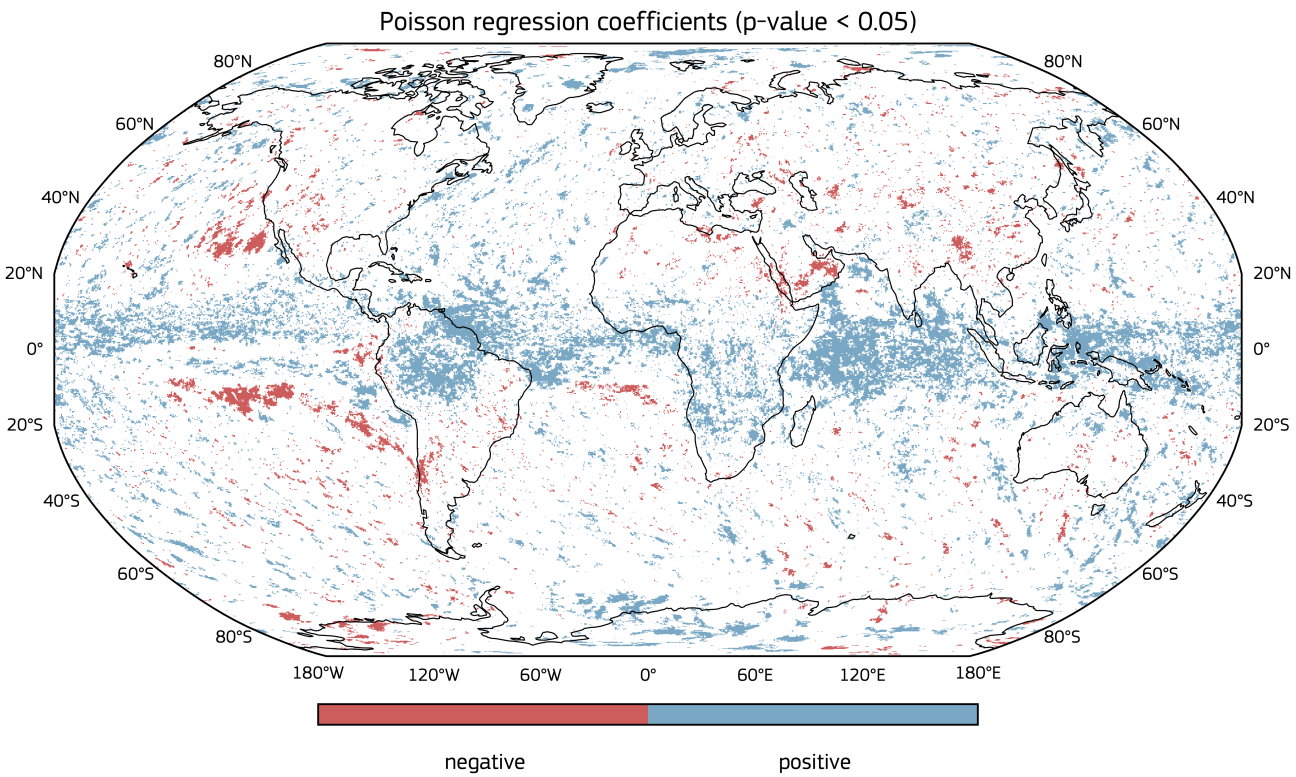

FIGURE 6 Grid points where the Poisson regression coefficients have a p-value <0.05 for the 0000 UTC to 0000 UTC accumulation period. Blue areas indicate an increasing trend in the number of extreme events (ERM >1), while red areas indicate a decreasing trend in the number of extreme events (ERM >1) from 1979 to 2023.

extremes has changed from 1979 to 2023. This is an important question to pose, as it is frequently heard—especially in the media—that the number of extremes is increasing. Figure 6 shows a map of the grid points for the 0000 UTC to 0000 UTC accumulation period where the positive or negative β_1 coefficients in the Poisson regression models have a p-value <0.05. The most striking consistent increasing trend is found across the majority of tropical areas between 20° N and 20° S. These trends are hypothesized to be questionable because ERA5 precipitation in these regions increases over time due to the assimilation of increasing amounts of microwave imager data (Soci et al., 2024). Increasing trends are also found scattered elsewhere. In terms of decreasing trends, there are two notable regions, one in the northeast Pacific (off Baja California) and a band in the southeast Pacific from approximately 10° S 155° W to the coast of Chile. These may relate to regions of high pressure or subsidence. Two further areas, over the southern Arabian Peninsula and southeast Asia, also had decreasing trends. Across Europe where most of the C3S activities are undertaken, there are, in general, more grid points with an increasing trend, but it is not possible to draw a firm conclusion on trends in extreme precipitation events in Europe based on this evaluation. Similar trend results were found for the 0600 UTC to 0600 UTC, 1200 UTC to 1200 UTC, and 1800 UTC to 1800 UTC accumulation periods.

4 | CONCLUSIONS

The aim of this article was to investigate further the ERM (Bosma et al., 2020) for communicating extreme precipitation by applying a modified version of the ERM to characterize extreme precipitation events around the globe in their climatological context. Using six case studies, which included convective systems, atmospheric rivers and tropical cyclones, the calculation of the ERM is illustrated and its meaning discussed. In the examples presented, a maximum ERM of 4 was found during Storm Daniel in Greece and in Tropical Cyclone Jasper in Australia, which implies that four times the mean historical RX1day precipitation (computed over 1991–2020) occurred. The identification of extreme precipitation events with the ERM has also been shown to have uses in climate monitoring activities by objectively identifying extreme events, which could prove useful for products such as the annual C3S ESOTC report. Furthermore, after extracting the number of extreme precipitation events with an ERM >1 per year at each grid point, a trend analysis was undertaken with Poisson regression to determine if the number of extreme events was increasing or decreasing with time. Results showed that the most widespread increasing trends occurred in the tropics, trends which are, however, considered questionable (Soci et al., 2024) and across the oceans, at least, arise from the assimilation of increasing amounts of microwave imager data. Conversely, decreasing trends were shown over the eastern Pacific Ocean and across southern parts of the Arabian Peninsula and southeast Asia. For Europe, there were more grid points exhibiting an increasing trend, but a firm conclusion on trends in extreme precipitation events cannot be drawn based on this evaluation.

It is hypothesized that the ERM could help more easily convey the extreme nature of a precipitation event to journalists and decision-makers and policymakers, rather than using return periods, standard deviations from the mean, or percentages of expected precipitation, as has been done in the past. In the future, there are many potential applications for the ERM, and four of these are outlined below. First, the ERM could be employed in diagnostic or evaluation studies of the ECMWF IFS and Artificial Intelligence/Integrated Forecasting System (AIFS), for example, to visualize weather forecasts in a climate context. A forecast example was presented for Hurricane Florence in 2018 in Bosma et al. (2020). This type of forecast information is of increasing relevance and interest to forecasters because of the severe impacts associated with extreme precipitation events. Research would be required though on how best to build a climate reference with model reforecasts that, for the IFS for instance, only exist on certain dates over the last 20 years. Furthermore, there is scope for the ERM to be applied to the IFS ensemble, such as by calculating the ensemble probability to have an ERM >1. Second, the temporal definition for an event across which the ERM is calculated could be extended from 24-h accumulation events to multi-day accumulations to capture longer-duration precipitation episodes (e.g., RX3day or RX5day) as in Bosma et al. (2020), or to different daily periods than the 0000 UTC to 0000 UTC, 0600 UTC to 0600 UTC, 1200 UTC to 1200 UTC, and 1800 UTC to 1800 UTC considered herein. Third, the ERM could be applied to other precipitation datasets, such as the Integrated Multi-satellitE Retrievals for the Global Precipitation Measurement (GPM) mission (IMERG; Huffman et al. (2020)), to compare and contrast with the trends found herein in ERA5. Lastly, it is also possible that the ERM could be applied to other variables like river discharge to characterize flooding severity. With the changes in extremes expected in a warming climate, the topic of effectively communicating extreme events will become of ever more importance, and the ERM will help to answer questions about how bad these events really are.

AUTHOR CONTRIBUTIONS

David A. Lavers: Conceptualization; formal analysis; investigation; methodology; writing – review and editing; writing – original draft; visualization. **Gabriele Villarini:** Conceptualization; methodology; writing – review and editing. **Hannah L. Cloke:** Conceptualization; methodology; writing – review and editing. **Adrian Simmons:** Conceptualization; methodology; writing – review and editing. **Nigel Roberts:** Methodology; writing – review and editing. **Anna Lombardi:** Visualization; writing – review and editing. **Samantha N. Burgess:** Conceptualization; writing – review and editing. **Florian Pappenberger:** Conceptualization; writing – review and editing.

ACKNOWLEDGEMENTS

The production of ERA5 and the contributions of David Lavers, Adrian Simmons, Anna Lombardi, and Samantha Burgess were supported by the Copernicus Climate Change Service, which is implemented by ECMWF on behalf of the European Union. Hannah Cloke acknowledges funding from the UKRI Natural Environment Research Council (NERC) The Evolution of Global Flood Risk (EVOFLOOD) project Grant NE/S015590/1. We are grateful to the comments of the Editor and three anonymous reviewers whose comments helped to improve this paper.

FUNDING INFORMATION

The contributions of David Lavers, Adrian Simmons, Anna Lombardi, and Samantha Burgess were supported by the Copernicus Climate Change Service, which is implemented by ECMWF on behalf of the European Union.

CONFLICT OF INTEREST STATEMENT

The authors declare that there are no conflicts of interest.

DATA AVAILABILITY STATEMENT

The ERA5 data used are freely available through the C3S Climate Data Store (https://cds.climate.copernicus.eu).

ORCID

David A. Lavers https://orcid.org/0000-0002-7947-3737
Gabriele Villarini https://orcid.org/0000-0001-9566-2370

REFERENCES

Blunden, J., Boyer, T. & Bartow-Gillies, E. (2023) State of the climate in 2022. *Bulletin of the American Meteorological Society*, 104(9), S1–S516. Available from: https://doi.org/10.1175/2023BAMSStateoftheClimate.1

Bosma, C.D., Wright, D.B., Nguyen, P., Kossin, J.P., Herndon, D.C. & Shepherd, J.M. (2020) An intuitive metric to quantify and communicate tropical cyclone rainfall Hazard. *Bulletin of the American Meteorological Society*, 101, E206–E220. Available from: https://doi.org/10.1175/BAMS-D-19-0075.1

Buontempo, C., Burgess, S.N., Dee, D., Pinty, B., Thépaut, J.-N., Rixen, M. et al. (2022) The Copernicus climate change service: climate science in action. *Bulletin of the American Meteorological Society*, 103, E2669–E2687. Available from: https://doi.org/10.1175/BAMS-D-21-0315.1

Hersbach, H., Bell, B., Berrisford, P., Hirahara, S., Horányi, A., Muñoz-Sabater, J. et al. (2020) The ERA5 global reanalysis. *Quarterly Journal of the Royal Meteorological Society*, 146(730), 1999–2049. Available from: https://doi.org/10.1002/qj.3803

Huffman, G.J., Bolvin, D.T., Braithwaite, D., Hsu, K.L., Joyce, R.J., Kidd, C. et al. (2020) Integrated multi-satellite retrievals for the global precipitation measurement (GPM) Mission (IMERG). *Advances in Global Change Research*, 1, 343–353. Available from: https://doi.org/10.1007/978-3-030-24568-9_19

Kim, H. & Villarini, G. (2024) Higher emissions scenarios lead to more extreme flooding in the United States. *Nature Communications*, 15, 237.

Kumar, P., Srivastava, S.S., Jivani, N., Varma, A.K., Yokoyama, C. & Kubota, T. (2024) Long-term assessment of ERA5 reanalysis rainfall for lightning events over India observed by tropical rainfall measurement Mission lightning imaging sensor. *Quarterly Journal of the Royal Meteorological Society*, 150(761), 2472–2488. Available from: https://doi.org/10.1002/qj.4719

Lave, T.R. & Lave, L.B. (1991) Public perception of the risks of floods: implications for communication. *Risk Analysis*, 11, 255–267. Available from: https://doi.org/10.1111/j.1539-6924.1991.tb00602.x

Lavers, D.A., Simmons, A., Vamborg, F. & Rodwell, M.J. (2022) An evaluation of ERA5 precipitation for climate monitoring. *Quarterly Journal of the Royal Meteorological Society*, 148(748), 3124–3137. Available from: https://doi.org/10.1002/qj.4351

Mazzoglio, P., Butera, I. & Claps, P. (2020) I2-RED: a massive update and quality control of the Italian annual extreme rainfall dataset. *Water*, 12(12), 3308. Available from: https://doi.org/10.3390/w12123308

Ralph, F.M., Dettinger, M.D., Cairns, M.M., Galarneau, T.J. & Eylander, J. (2018) Defining "atmospheric river": how the glossary of meteorology helped resolve a debate. *Bulletin of the American Meteorological Society*, 99, 837–839. Available from: https://doi.org/10.1175/BAMS-D-17-0157.1

Salas, J. & Obeysekera, J. (2014) Revisiting the concepts of return period and risk for nonstationary hydrologic extreme events. *Journal of Hydrologic Engineering*, 19, 554–568. Available from: https://doi.org/10.1061/(ASCE)HE.1943-5584.0000820

Smith, J.A., Cox, A.A., Baeck, M.L., Yang, L. & Bates, P.D. (2018) Strange floods: the upper tail of flood peaks in the United States. *Water Resources Research*, 54, 6510–6542. Available from: https://doi.org/10.1029/2018WR022539

Soci, C., Hersbach, H., Simmons, A., Poli, P., Bell, B., Berrisford, P. et al. (2024) The ERA5 global reanalysis from 1940 to 2022. *Quarterly Journal of the Royal Meteorological Society*, 150(764), 1–35. Available from: https://doi.org/10.1002/qj.4803

Thompson, V., Kennedy-Asser, A.T., Vosper, E., Lo, Y.T.E., Huntingford, C., Andrews, O. et al. (2022) The 2021 western

North America heat wave among the most extreme events ever recorded globally. *Science Advances*, 8(18), eabm6860.

Villarini, G., Goska, R., Smith, J. & Vecchi, G. (2014) North Atlantic tropical cyclones and U.S. flooding. *Bulletin of the American Meteorological Society*, 95(9), 1381–1388 https://journals.ametsoc.org/view/journals/bams/95/9/bams-d-13-00060.1.xml.

You, Y., Ting, M. & Biasutti, M. (2024) Climate warming contributes to the record-shattering 2022 Pakistan rainfall. *Npj Climate and Atmospheric Science*, 7, 89. Available from: https://doi.org/10.1038/s41612-024-00630-4

Zhang, X., Alexander, L., Hegerl, G.C., Jones, P., Tank, A.K., Peterson, T.C. et al. (2011) Indices for monitoring changes in extremes based on daily temperature and precipitation data. *Wiley Interdisciplinary Reviews: Climate Change*, 2(6), 851–870.

SUPPORTING INFORMATION

Additional supporting information can be found online in the Supporting Information section at the end of this article.

How to cite this article: Lavers, D. A., Villarini, G., Cloke, H. L., Simmons, A., Roberts, N., Lombardi, A., Burgess, S. N., & Pappenberger, F. (2025). How bad is the rain? Applying the extreme rain multiplier globally and for climate monitoring activities. *Meteorological Applications*, *32*(2), e70031. https://doi.org/10.1002/met.70031